JOURNAL OF PROPULSION AND POWER
Vol. 17, No. 6, November–December 2001

Effect of Flame-Holding Cavities on Supersonic-Combustion Performance

Ken H. Yu*
University of Maryland, College Park, Maryland 20742
and
Ken J. Wilson† and Klaus C. Schadow‡
Naval Air Warfare Center, China Lake, California 93555

An experimental study was performed to evaluate the flame-holding and mixing enhancement characteristics of supersonic reacting flow over acoustically open cavities. Several configurations of acoustically open cavities were placed inside a supersonic-combustion duct just downstream of the fuel injection ports. The resulting changes in flame behavior and combustion characteristics were assessed using schlieren visualization of the unconfined flow and wall pressure measurements of the confined flow along the duct. The results were then compared with the baseline case, which used no cavity. Although the cavities improved the combustion performance from the baseline, the amount of enhancement was dependent on the particular shape of the cavity as well as the flow conditions. Certain cavity configurations that were strategically placed inside the combustion duct led to a faster increase in the axial pressure force. The data showed that the recovery temperature was higher and the total pressure profile was more uniform at the exit plane, suggesting enhanced volumetric heat release and faster mixing associated with the cavity- influenced flowfield.

I. Introduction

FUEL-AIR mixing in an airbreathing engine becomes increasingly inefficient at higher velocity, hence requiring a longer combustor length. Although this is caused by the reduced flow residence time inside the combustor and the compressibility effect that adversely affects the rate of mixing,[1–3] a short combustor length is desirable because the thrust-to-drag ratio of an engine is roughly proportional to the ratio between the combustor diameter and length. To generate practically useful thrust to drag, length-to-diameter ratio of a combustor should be sufficiently small. In compact engines with small diameter, however, the ratio will be relatively large unless the combustor length can be reduced accordingly.

In an effort to reduce the combustor length, acoustically open cavities were placed inside a supersonic-combustion duct setting up a recirculating flow suitable for flame holding. An acoustically open cavity is characterized by a cavity length-to-depth ratio sufficiently small not to allow shear-layer reattachment on the cavity floor. The limiting ratio for acoustically open cavities depends on the flow conditions and is typically less than 10. Because the pressure drop associated with acoustically open cavities is relatively small, strategically placed cavities in the combustor could provide practical benefit by increasing the flow residence time and setting up flame holding. Flame-holding characteristics of various cavities have been exploited in the past studies involving subsonic combustors. For instance, Huellmantel et al.[4] compared flame-holding capability of various shaped cavities for propane-air flames at low subsonic speed. Also, the "trapped-vortex" concept, which utilizes a stationary vortex developing inside a small-aspect-ratio cavity, has been explored for stable flame holding in gas turbines.[5,6]

In high-speed propulsion an integrated fuel injector/flame holder using simple cavities is one of several new concepts that may provide potential performance benefit for net thrust.[7] Recent studies investigated the effect of flame-holding cavities in supersonic streams[8,9] and examined the drag[10] and stability characteristics[11] of flames. Such a technique would be particularly useful for stable flame holding at low equivalence ratio and for minimizing the effect of shock trains in dual-mode operation. Although pilot flames anchored in the cavity are interesting as they can shorten the ignition-delay time of fuel-air mixture, acoustic characteristics of cavity can also be optimized to excite the shear flow and enhance turbulent mixing.

Flow-induced cavity resonance, which may develop spontaneously under certain conditions,[12] is another interesting feature of a cavity flow. The effect of cavity resonance on a Mach 2 jet shear layer is shown in Fig. 1. Under certain conditions[13,14] the resonance causes periodic shedding of organized structures that can be used to control mixing. For instance, in a study of cavity-excited jets, it was shown that cavity geometry could be tuned to manipulate periodic shedding of lateral vortices, ultimately controlling the rate of entrainment and turbulent compressible mixing.[15] Also, it may be beneficial to use multiple cavities side by side for controlling their interaction.[16] In such a configuration stable cavities could be used for flame-holding purpose, whereas other unstable cavities would enhance turbulent mixing and combustion.

Therefore, combustor wall cavities that are strategically placed can provide many potential benefits that include mixing improvement as well as stable flame holding. The present contribution comprises an experimental investigation in which several cavity configurations were incorporated in the design of a supersonic combustion duct. The configurations were selected from a previous study[9] in which the cavity parameters were systematically varied. The objective was not only to better understand the physical mechanisms that caused the performance change, but also to assess quantitatively and rank the effectiveness of various cavities for propulsion applications.

II. Nonreacting Flow Experiments

Flow oscillations induced by cavities can be used to generate large-scale lateral vortices that increase the rate of entrainment and dominate turbulent compressible mixing and combustion. The spreading rate of the excited shear layers[17] is substantially higher than the natural growth rate of turbulent compressible shear layers,[1,18–21] which is represented by the shaded region in Fig. 2.

Presented as Paper 99-2638 at the AIAA/ASME/SAE/ASEE 35th Joint Propulsion Conference and Exhibit, Los Angeles, CA, 20–23 June 1999; received 27 October 2000; revision received 11 January 2001; accepted for publication 23 January 2001.

*Associate Professor, Department of Aerospace Engineering. Senior Member AIAA.
†Aerospace Engineer, Research Department.
‡Staff Scientist, retired.

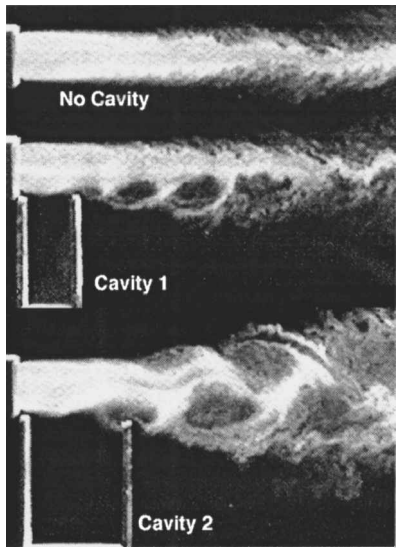

Fig. 1 Planar Mie-scattering images of pressure-matched Mach 2 jets discharging over acoustically open cavities that created flow-induced cavity resonance.

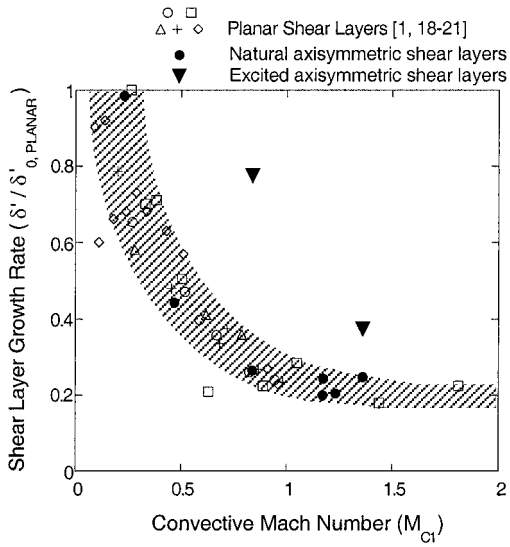

Fig. 2 Normalized growth rate of natural and excited shear layers.[1,18–21]

Previously it was shown that the amount of increase was dependent on oscillation frequency with the maximum increase occurring near the jet preferred mode.[17]

Earlier work on the jet oscillation frequencies was conducted by Rossiter[12] who considered flow-induced cavity resonance, by Powell[22] who investigated screech tones, and by Tam[23] and Tam and Block[24] who calculated the acoustic normal modes of rectangular cavities. In general, the oscillation frequencies f can usually be predicted by considering both the acoustic eigenmodes of the cavity and the coupled acoustic-convective mode of the shear flow hydrodynamic disturbances.[17] For instance, the acoustic eigenmodes are given by

$$f_{mn}L/U = (c/2U)\sqrt{(m-1)^2 + \left(n-\tfrac{1}{2}\right)^2 (L/D)^2} \qquad (1)$$

where c is the speed of sound in the cavity, U the freestream velocity, L the cavity length, D the cavity depth, and the ordered integers (m, n) denote the longitudinal and the transverse mode numbers, respectively. On the other hand, the coupled acoustic-convective mode can be written in the Rossiter form[12] as

$$\frac{f_n L}{U} = \frac{n-\gamma}{U/c + 1/\kappa} \qquad (2)$$

where γ denotes the phase lag effect, which is a weak function of L/D, and κ is the ratio between the convection velocity of the disturbance and the freestream velocity. A recent study by Raman et al.,[25] however, also indicated that jet-cavity interaction can produce a unique set of tones that are different from the traditional frequencies depending on the cavity depth.

In the present work the oscillation frequencies were measured during cold flow tests using an open duct configuration. Figure 3 shows the open duct configuration and the schematic illustration of the base flowfield in the presence of fuel injection and subsequent flames. A two- dimensional sharp-corner nozzle was used to expand high-pressure air from the storage tank, setting up a supersonic jet with aspect ratio of 2 at the nozzle exit. The nozzle was operated at the design Mach number of 2.0 at the exit, and the air jet was discharged over a flat plate, forming a supersonic wall jet at the test section. A separate gas generator supplied high-temperature combustion products to the test section to simulate the fuel injection process. The products were injected from the bottom wall using circular tube injector ports that were flush mounted. Three injector ports were used in the open duct configuration, whereas only two injector ports were used in the ducted experiments, which will be presented in the later section. Because the injectors were pointed at 45 deg with respect to the bottom wall in the flow direction, the injector exit became elliptic in shape.

The flow conditions for the six cases presented in this paper are shown in Table 1. For most of the experiments, the static temperature

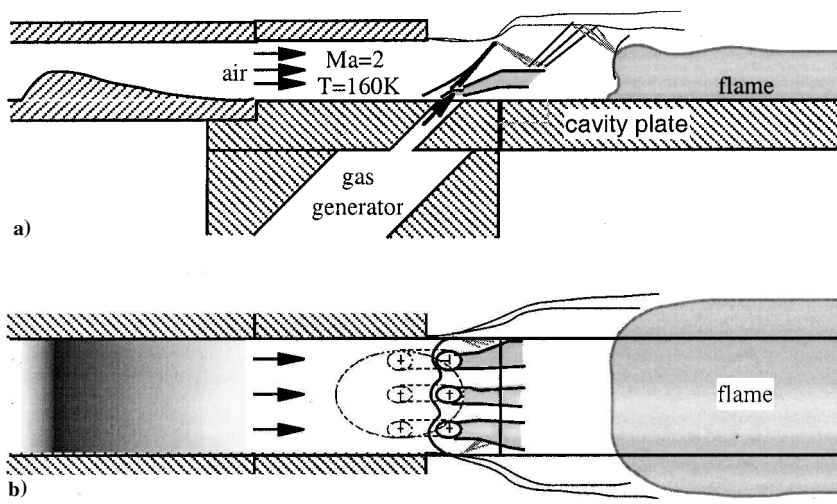

Fig. 3 Test setup and schematic diagram of the flowfield without the side and top wall: a) side and b) top view.

Table 1 Inlet and gas generator flow conditions

	Inlet airflow				Gas generator products (fuel)		
Case	Ma	T, K ($\pm 6°$)	p, psi (± 0.1)	m_{air}, Kg/s	Composition	$T_{0,g}$, K ($\pm 80°$)	m_{inj}, kg/s
N1	2.0	160	13.7	0.50	——	——	0
N2	2.0	160	13.7	0.50	$0.35H_2O + 0.65N_2$ (Simulated Fuel)	2400	0.017
F3	2.0	160	13.7	0.50	$0.28C_2H_4 + 0.36CO_2 + 0.36H_2O$	2600	0.017
C4	2.0	160	21.0	0.77	$0.33C_2H_4 + 0.33CO_2 + 0.33H_2O$	2200	0.010
C5	2.0	160	27.3	1.00	$0.33C_2H_4 + 0.33CO_2 + 0.33H_2O$	2200	0.010
C6	2.0	160	21.0	0.77	$0.4C_2H_4 + 0.3CO_2 + 0.3H_2O$	2100	0.011

Table 2 Resonant frequencies under case N1 conditions

Cavity configuration	L/D	f, kHz
Baseline	——	——
No. 1	0.5	——
No. 2	1	——
No. 3	2	21.5
No. 4	3	23.5
Inclined	~5	——
No. 2 + No. 4	——	23.5
No. 3 + No. 3	——	21.5
Inclined + No. 3	——	——

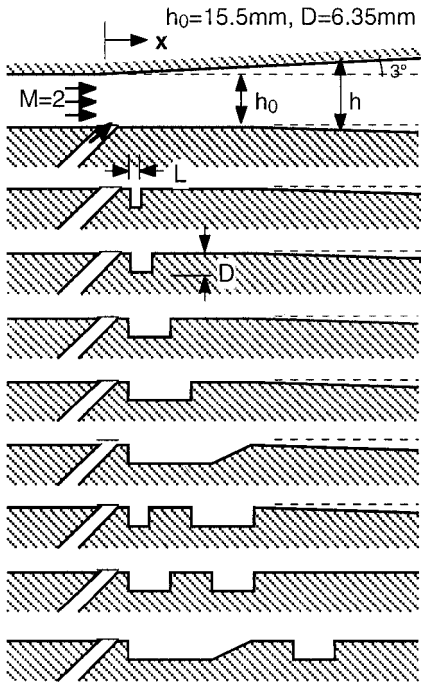

Fig. 4 Various cavity configurations.

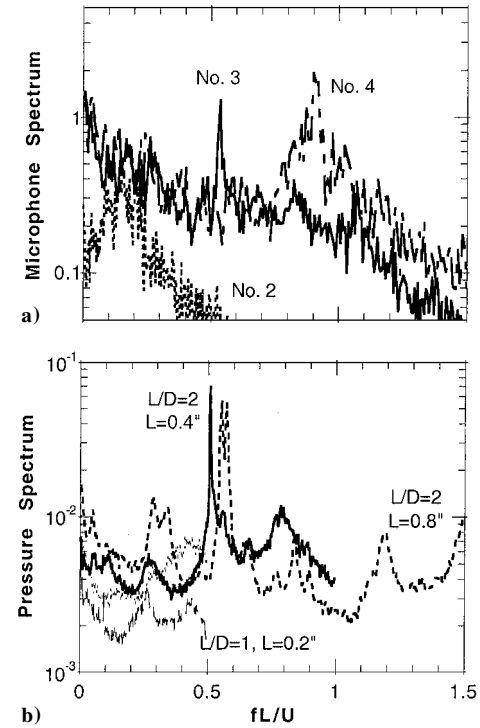

Fig. 5 Typical cavity pressure spectra a) without and b) with the combustor duct in place.

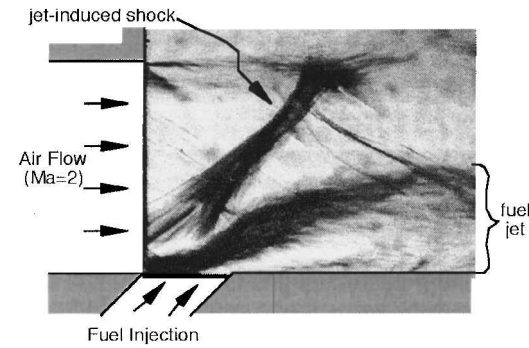

Fig. 6 Spark schlieren image of fuel jet injection into the supersonic stream.

T and the static pressure p at the inlet entrance were deduced from the stagnation parameters that were measured. This practice was acceptable because the inlet nozzle had been characterized with actual measurements of stagnation and static conditions, which previously verified the proper relation. The first two cases, N1 and N2, are for nonreacting (N) flow experiments. Case F3 is for the open-flow flame (F) experiment, discussed in the next section, whereas the other three cases are for the combustor (C) experiments shown in the following section. The stagnation temperature was calculated on the basis of measured stagnation pressure and the reactant flow rates. The specified error values represent the maximum of statistical scatter and uncertainties in repeated experiments. All of the flow rates were metered by choked orifices.

A summary of the cavity configurations is provided in Table 2 and Fig. 4. The excitation frequencies were measured under case N1 flow conditions. Figure 5 shows typical pressure spectra obtained either with a microphone without the duct or with a pressure transducer flush mounted to the duct. Because the oscillations were measured without fuel injection, the frequency values represent only a reference measure suggesting the cavity stability characteristics. No organized oscillations were detected inside the no. 1, no. 2, and inclined cavities, whereas no. 3 and no. 4 cavities resulted in relatively weak and strong acoustic oscillations, respectively. For the double-cavity configuration using two no. 3 cavities, the pressure inside the trailing cavity displayed a much higher degree of coherence. The oscillations were stronger when the flow was confined as the duct prevented the flow entrainment and enhanced the acoustic feedback inside the cavity.

Figure 6 shows a spark schlieren image of the simulated fuel injection in case N2. To eliminate the afterburning that can interfere

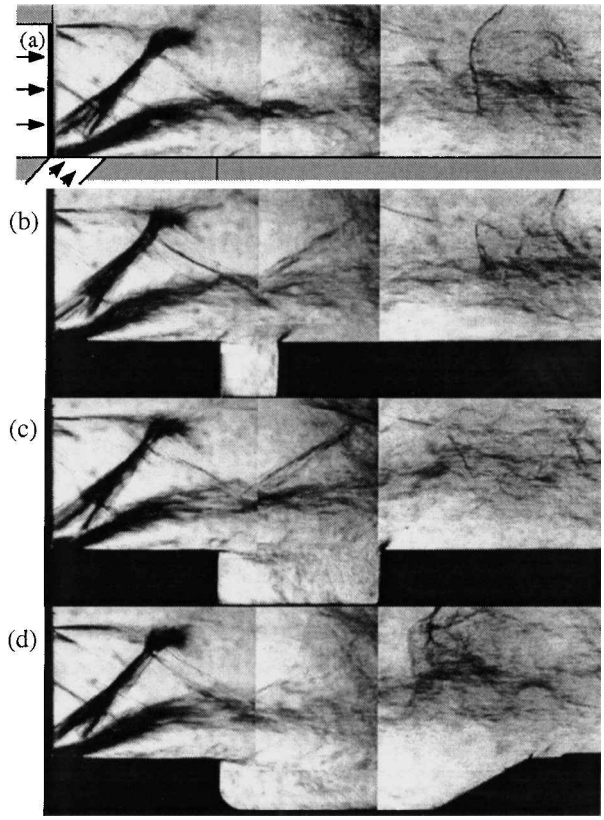

Fig. 7 Spark schlieren images of fuel injection in various configurations: a) baseline, b) no. 2 cavity, c) no. 4 cavity, and d) inclined cavity.

with the flowfield visualization, the gas generator was operated at a stoichiometric condition. For the schlieren stop a small aperture was used instead of a knife edge, making the density gradient in the radial direction visible. Some of the characteristic structures including fuel-jet shear layers and jet-induced shock structures are shown in the image. Figure 7 shows spark schlieren images corresponding to various configurations. Several images taken from respective locations in the flowfield were put together to construct an ensemble view of each configuration. Although it was difficult to isolate clear qualitative difference between the various configurations, the images nevertheless showed a subtle difference in temporal structures. With the use of unstable cavities, the downstream shock structure became more unsteady and irregular. Also, the shock structure was often observed slightly further upstream with the use of the cavities. Such a shock structure was shown to be associated with the flame initiation in the reacting case, which is presented in the next section. For the inclined-cavity case in particular, the injected fuel jets appeared to be pulled more toward the cavity floor than in other cases. The result is consistent with the expectation as this represented the longest single cavity length employed in this study.

III. Open-Flame Experiments

In the flame experiments that were conducted without the top and side walls, excess ethylene from the gas generator was used to set up reacting flow downstream (case F3). In the baseline configuration the flames were observed detached from the injectors and initiated about 10 orifice diameters downstream from the point of injection. The flames appeared to be stabilized behind a shock structure. Although the short-time-exposed flame images revealed that the afterburning was very unsteady, the average behavior of the flames was highly reproducible from run to run. Figure 8 shows the time-averaged flame images taken from the side that were converted into iso-intensity contours. Except for the inclined cavity, bright emission was observed inside most cavities, indicating reaction in the recirculating flow. With the inclined cavity the fuel jets appeared to be partially impinging on the inclined surface causing more drastic changes in the flame structure.

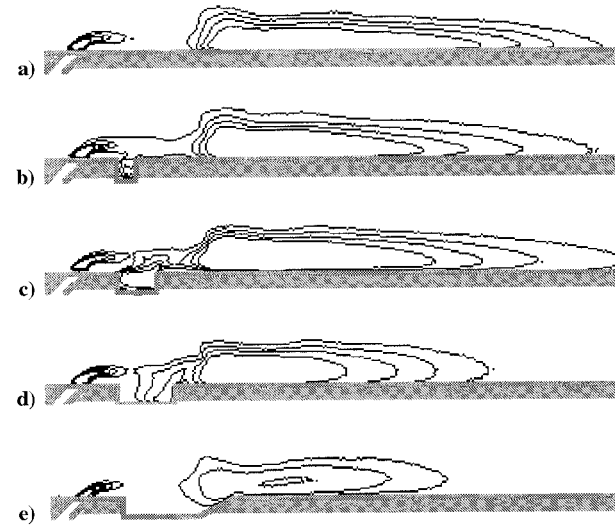

Fig. 8 Iso-intensity luminosity contours of time-averaged flame images for a) baseline, b) no. 2, c) no. 3, d) no. 4, and e) inclined cavity.

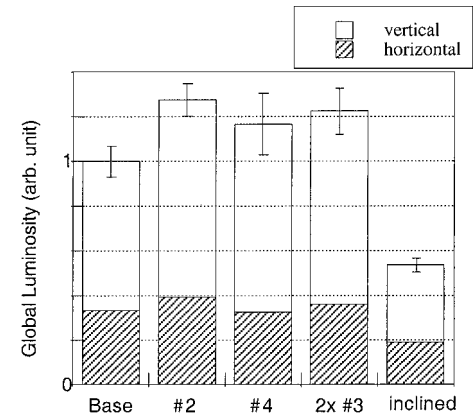

Fig. 9 Comparison of global emission intensity measured from horizontal (side) and vertical (top) directions.

In all of the images, the onset of main flow ignition occurred at a similar location, which suggests that the flame ignition was related to the subsonic transition of underexpanded injectant flows. To quantify the effect of cavities on flame length and intensity, the flame luminosity in the visible range was measured, and the axial variation of local intensity was considered. Although the flame luminosity is not a direct measure of the heat-release characteristics, it nevertheless provides valuable information about the flame structure.

To make an overall quantitative comparison, both measurements from top and side were averaged, and the results are presented in Fig. 9. The weighting factor between the two measurements was selected on the basis of the aspect ratio for the freestream jet. The results show that the overall flame intensity can be manipulated with the use of cavities. Depending on particular cavity used, the change in overall luminosity could be from 28% increase to 46% reduction. The preceding results suggest that it is possible to affect the combustion efficiency using various cavities in the flow. For instance, if the general nature of the turbulent flames were similar with or without the cavities, the luminosity measurements in these tests would be related to the relative combustion intensity.

Figure 10 shows the comparison of relative flame length between the various cases. The relative flame length was obtained by measuring the length from the injector location to the downstream location where local emission intensity dropped to one-fifth of the maximum local emission intensity in the baseline case. The threshold value of one-fifth was arbitrarily chosen based on the background noise intensity and the repeatability of reduced data. The marked error bars reflect the flame length measurements when

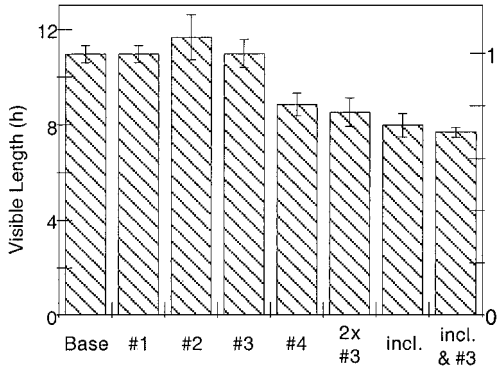

Fig. 10 Visible flame length for various configuration measured from axial luminosity data.

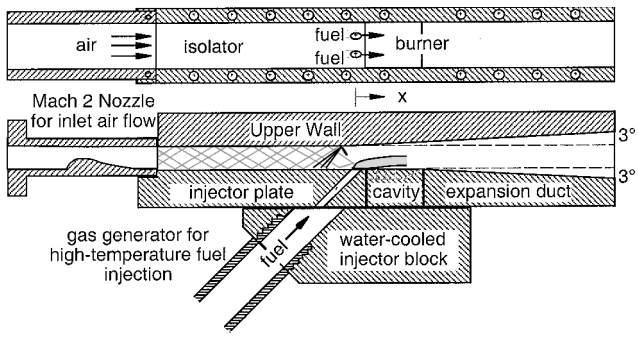

Fig. 11 Supersonic combustion rig simulating dual-mode system.

the threshold value was changed by ±5%. The results showed that the flame length as just defined could be reduced by as much as 30% when certain cavities were used. Because the observed flame characteristics such as length and intensity were substantially different in some of the cases, it became meaningful to further assess the effect of cavities in a confined supersonic combustor.

IV. Combustor Experiments

To quantify the potential performance gain of utilizing the cavities, some of the configurations from the open flame experiments were selected and tested in the combustor experiments. Figure 11 shows the cross-sectional view of the combustion rig that simulated dual-mode scramjet system.[26] It consisted of a constant-area isolator section with the aspect ratio of 2, which was followed by an expanding-area combustor. As before, the cavity plate was positioned just downstream of the fuel injection ports. However, only two injection ports were used in the combustor experiments.

First, wall pressure distribution in the flow direction was measured by sampling the pressure on the top wall along the centerline. Figure 12 shows the mean amplitude of pressure along the upper wall for the baseline configuration and the inclined cavity configuration, with both simulated and actual fuel injection cases. The axial distance from the fuel injection point x is normalized by the inlet-duct height h_0 and is shown in the abscissa, while the wall pressure p_w is normalized with the stagnation pressure p_0 and is shown in the ordinate. The pressure in the combustor increases as a result of additional mass flux from fuel injection as well as the heat release associated with the combustion of the fuel. In the simulated-fuel-injection case (NR) only the first is responsible for the pressure change as there is no reaction inside the combustor. Thus, the difference in the wall pressure between the baseline and the inclined-cavity configurations comes from the geometry change only. Except in the narrow region near the cavity plate, where the effect of geometry change is communicated to the upper wall by the supersonic flowfield, the pressure amplitude was nearly identical for the two configurations with the simulated fuel injection.

With the actual fuel injection (R), however, the difference is magnified by the change in combustion efficiency between the two configurations. The combustor pressure in the baseline configuration increased with the actual fuel injection, as the presence of exothermic reaction added heat to the flow. Interestingly, with the use of the cavity, this increase in the wall pressure became even higher, indicating more efficient heat release inside the combustor.

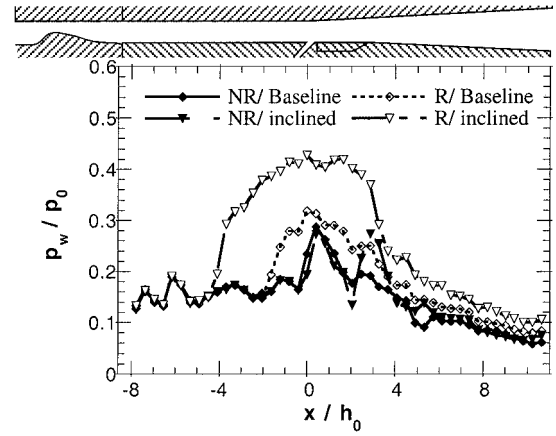

Fig. 12 Average wall pressure distribution for selected cases: NR, nonreacting case and R, reacting case.

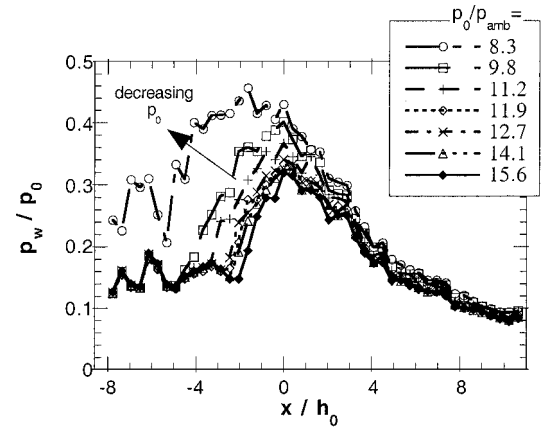

Fig. 13 Effect of pressure increase on combustor wall pressure distribution.

From Fig. 12 it is evident that the location of the jet-induced shock moved further upstream when the combustor pressure was increased with the cavity. Figure 13 shows the comparison of wall pressure distribution for various combustor pressures in the baseline configuration. The relative pressure ratio was modified by changing the freestream stagnation pressure, while holding the fuel injection condition constant. From this plot the effect of combustor pressure on the shock location can be deduced. As the relative amplitude of the combustor pressure increased, the shock location appeared to move further and further upstream. This result also indicates the thickening of the boundary layer associated with the combustor pressure increase.

Figure 14 shows the wall pressure distribution for various cavity configurations that were compared against the baseline. The error bars on the baseline case data represent the amount of rms fluctuations at each measuring station. When a cavity was utilized, the combustor pressure became substantially higher than in the baseline case. The comparison between different cavity configurations was made under two different freestream conditions. When $p_0/p_{amb} = 11.9$ (case C4), the maximum value of p_w/p_0 increased by 50–60% depending on the cavity configuration. For $p_0/p_{amb} = 15.6$ (case C5) the maximum pressure was about 35–54% higher than the baseline. These results are presented in Fig. 15a, which shows the maximum wall pressure along the combustion duct. The dotted line represents the reference static pressure of a choked airflow. The maximum wall pressure approached this value

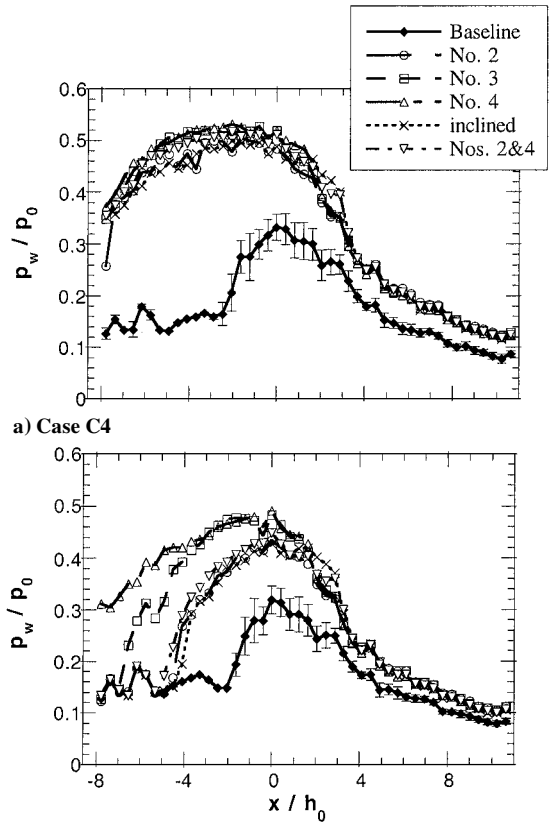

Fig. 14 Changes in wall pressure distribution when various cavities are used.

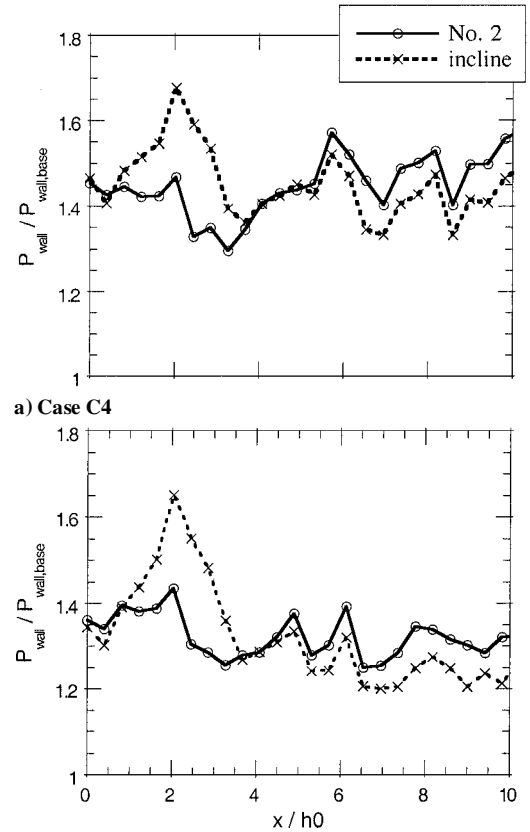

Fig. 16 Relative wall pressure increase on the expanding duct.

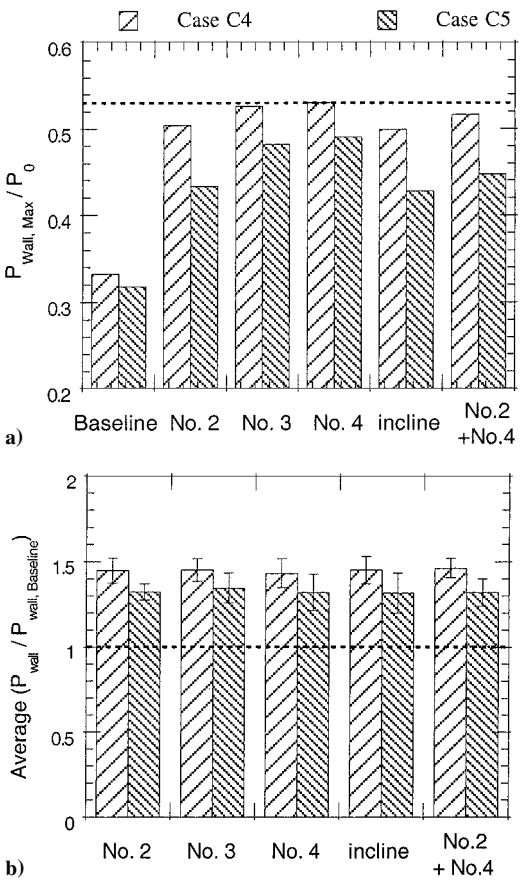

Fig. 15 Comparison of wall pressure: a) maximum pressure observed and b) relative pressure increase with respect to the baseline configuration.

for longer cavities but still remained below this value indicating supersonic nature of the flow. The no. 4 cavity, which produced the highest oscillation amplitude in the nonreacting experiments, also resulted in the highest maximum wall pressure in the combustor experiments. Figure 15b shows the relative increase in the wall pressure, which was averaged over the expanding surface only. Although there was a substantial increase in the combustor pressure from the baseline case, the average amount of increase appeared to be about the same regardless of the cavity configuration. This appears to be related to the fact that the combustion duct was long enough in these experiments to accommodate complete reaction inside the duct once flame holding was established. The use of cavities, by providing a stable flame holding, reduced the amount of unburned fuel escaping the combustion duct. The amount of scatter in the averaged data was very low despite much higher value of uncertainties indicated by the error bars. For instance, the average amount of relative pressure increase from the corresponding baseline configuration value was $45 \pm 1\%$ for the case C4 conditions and $33 \pm 1\%$ for the case C5 conditions.

Figure 16, on the other hand, shows the relative increase in the wall pressure as a function of the axial distance from the fuel injection location. Only two sets of data are shown here to highlight the difference between various configurations. Although the amount of pressure increase averaged over the diverging portion of the duct was nearly identical for different cavities, certain cavity configurations, such as the inclined cavity or the combination cavities arranged in tandem, caused much higher pressure increase initially, at locations close to the fuel injection point. This suggests that the heat-release process was volumetrically more efficient in these cases, causing a relatively high initial pressure rise.

To quantify the change in pressure force exerted on the upper wall, the axial component of wall pressure amplitude was integrated over the expanding surface. The results were also normalized using the baseline case, and they are shown in Fig. 17 as a function of the expansion duct length. The axial force F in Fig. 17 denotes the total force on the expanding wall, integrated up to the axial location x.

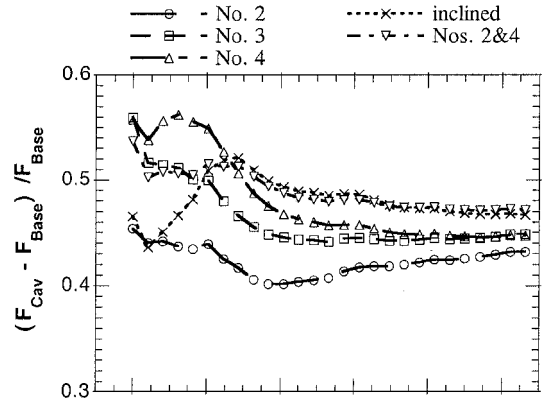

a) Case C4

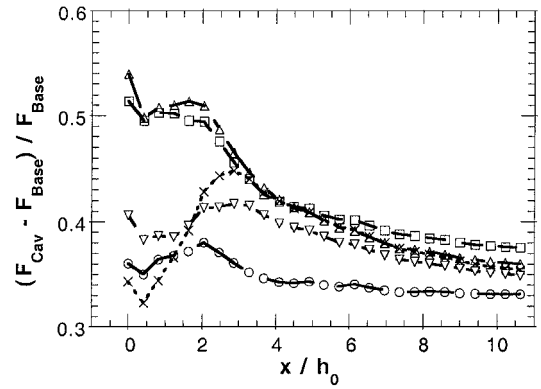

b) Case C5

Fig. 17 Increase in the axial force on the expanding surface relative to the baseline.

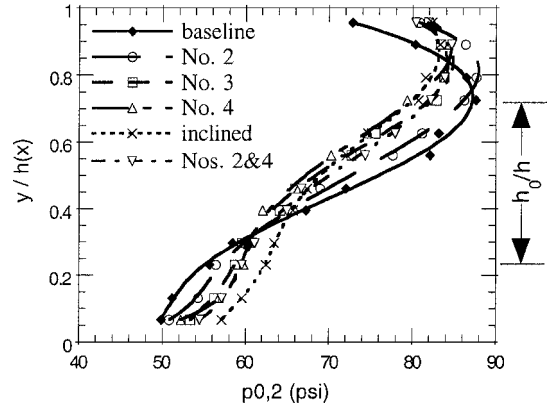

a) Case C4

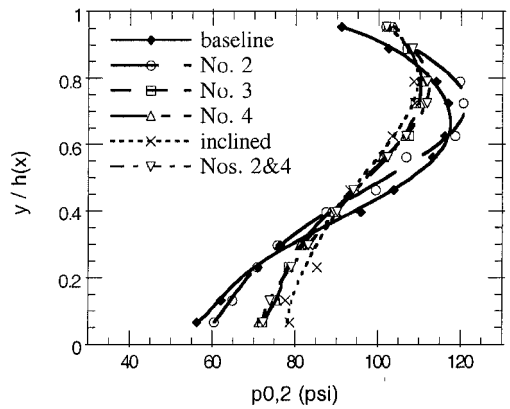

b) Case C5

Fig. 18 Measured total pressure profiles near the duct exit at $x/h_0 = 10.6$. The initial duct height h_0 at fuel injection location $x = 0$ is shown on the right vertical axis for reference.

The pressure amplitude was affected severely by the cavity geometry, particularly between zero and three duct height downstream of the fuel injection point. For relatively short duct length the amount of increase in axial force would be substantially different depending on the cavity configuration. However, as the expansion duct becomes longer, the relative increase in the axial force converges to a similar value regardless of the cavity configuration, in a consistent trend as that illustrated in Fig. 15b. This implies that while the overall heat release inside the combustor can be increased by utilizing any configuration of the flame-holding cavities the volumetric heat release along the axial direction could be optimized by the proper choice of the cavity shape. For axial force consideration, particularly under case C4 condition, the inclined cavity and the configuration with the cavities in tandem were most effective. Also, under case C5 condition no. 3 cavity and the inclined cavity were most effective.

To deduce the physical mechanisms responsible for the increase in the combustor pressure and the corresponding axial force, transverse profiles of the exit flow were measured at 10.6 duct heights downstream from the injection location ($x/h_0 = 10.6$). All of the transverse measurements were made along the minor axis of the duct, aligned with the plane that is equally distanced from the two injector ports. Figure 18 shows the measured total pressure profiles for two different freestream conditions. For both conditions the profiles were somewhat asymmetric showing pressure deficit on the lower wall, from which fuel was injected. With the use of the cavities, the total pressure profile became more uniform indicating faster mixing. In general, longer cavities made the profiles more uniform. However, this could also be indicative of the fact that the longer cavities would incur a higher pressure drop. On the basis of the present data, the inclined cavity produced a more uniform profile than other cavities.

Figure 19 shows the recovery-temperature profiles at the same location. The temperature measurements were made using a stationary thermocouple, which was traversed across the flow after each measurement. The baseline case data show a relatively thick

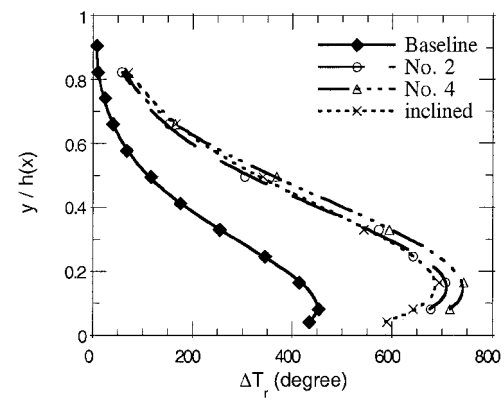

a) Case C4

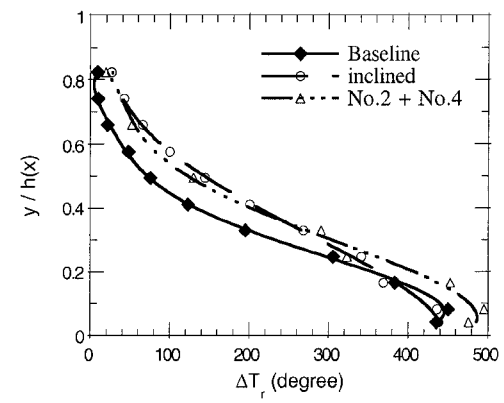

b) Case C5

Fig. 19 Recovery temperature profiles near the duct exit at $x/h_0 = 10.6$.

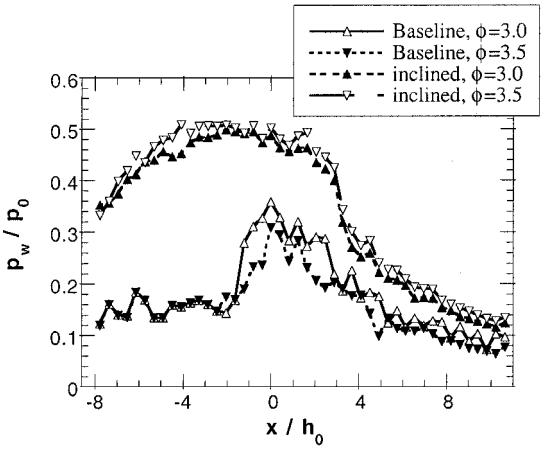

Fig. 20 Effect of gas generator equivalence ratio in two selected configurations (cases C4 and C6).

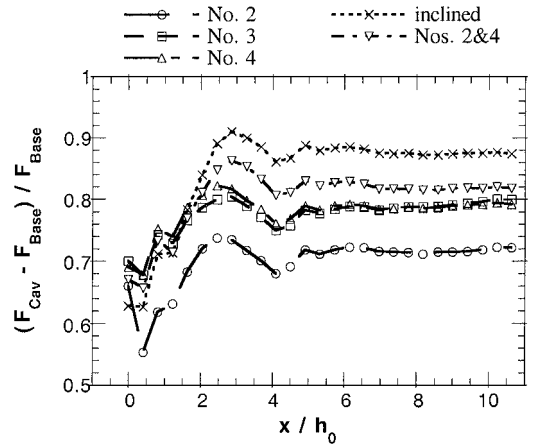

Fig. 21 Increase in the axial force associated with the cavity when the baseline performance is poor (case C6).

thermal boundary layer on the upper wall, which implies a limited penetration of the injected fuel into the freestream. With the cavities the thermal layer profile is not only more developed, but the temperature is also much higher than the baseline case. The recovery temperature was higher with the acoustically unstable cavities than with the stable ones. In all of the cases that utilized cavities, the combustor exit pressure profiles were more uniform and the recovery temperature higher suggesting better mixing and enhanced combustion efficiency.

Figure 20 compares the effect of cavities in two different cases using the baseline and the inclined cavity configurations. The fuel-air ratio was modified from case C4 condition ($\phi = 3.0$) by increasing the gas generator equivalence ratio while holding the mass flux constant. Thus, in case C6 ($\phi = 3.5$) the total amount of fuel available for combustion was greater although the fuel was injected into the combustor at slightly lower temperature. For the baseline configuration, however, even though the fuel flux was greater in case C6 the resulting combustor pressure was lower than that in case C4. This result can be interpreted as the reflection of relatively poor combustion efficiency in the baseline configuration, which becomes even worse with the lowering of fuel temperature. However, when the inclined cavity configuration was subjected to the same flow condition, the proper trend was restored. As expected, when mixing was enhanced with the cavity, the case C6 condition with the greater amount of fuel flux resulted in higher combustor pressure. This result illustrates the effectiveness of wall cavities in enhancing overall combustion performance as well as the volumetric heat release.

Figure 21 shows the relative increase in the axial force associated with the use of cavities for the case C6 condition. Because of relatively inefficient combustion under the baseline configuration, the increase in case C6 is significantly higher than in the preceding cases, ranging from 70 to 90% enhancement. Again, the inclined cavity produced the highest enhancement in axial force, followed by the two cavities in tandem and then long and short cavities in that order.

V. Conclusions

An experimental study was conducted to evaluate the flameholding and mixing enhancement characteristics of supersonic reacting flow over acoustically open cavities. Several wall cavities having various size and aspect ratios were subjected to supersonic open-flow flame experiments. The flames were created with high-temperature fuel-rich products injected into a Mach 2 airstream at a 45-deg angle, and the effect of cavities was investigated by placing the selected cavities just downstream of the fuel injection point. The results showed that cavities with a short aspect ratio provided good flame holding, whereas those with a relatively long aspect ratio shortened the flame length substantially via acoustic excitation. Subsequently, some of the selected cavity configurations were placed inside a supersonic combustion duct. For each configuration the axial wall pressure distribution was measured along the duct, and the stagnation pressure profile and the recovery temperature profile were obtained at the duct exit in the transverse direction. The results were then compared against the baseline case with no cavity. In all cases that utilized cavities, the combustor pressure and the exit recovery temperature were substantially increased, suggesting enhanced volumetric heat release. The total pressure profile also became more uniform at the exit, indicating better mixing. The measured wall pressure on the expansion surface was increased significantly from the baseline case depending on the flow conditions and the cavity configuration.

The results indicated that the volumetric heat release could be increased with certain cavities strategically placed inside the combustor. Among the cavity configurations used in this study, some provided consistently superior performance in terms of flow profile uniformity and the pressure amplitude on the expansion surface. In consideration of the pressure force exerted on the expansion surface, the inclined cavity and the configuration utilizing two cavities in tandem produced the best results among those configurations studied. At the same time, however, these were the longest cavities considered in the study, and thus they are most likely to suffer from adverse effects caused by forces exerted on the cavity walls. For practical considerations, therefore, one must evaluate the positive effect of cavity-enhanced combustion efficiency against the negative effect caused by to cavity-induced drag.

Acknowledgments

This research was supported by Office of Naval Research and Naval Air Warfare Center In-House Lab Independent Research Program. The initial work on supersonic mixing enhancement using cavities was sponsored by Office of Naval Research, Propulsion Research Program, with Gabriel Roy as the Program Officer.

References

[1] Papamoschou, D., and Roshko, A., "The Compressible Turbulent Shear Layer: an Experimental Study," *Journal of Fluid Mechanics*, Vol. 197, 1988, pp. 453–477.

[2] Bogdanoff, D. W., "Compressibility Effects in Turbulent Shear Layers," *AIAA Journal*, Vol. 21, No. 6, 1983, pp. 926, 927.

[3] Gutmark, E. J., Schadow, K. C., and Yu, K. H., "Mixing Enhancement in Supersonic Free Shear Flows," *Annual Review of Fluid Mechanics*, Vol. 27, 1995, pp. 375–417.

[4] Huellmantel, L. W., Ziemer, R. W., and Cambel, A. B., "Stabilization of Premixed Propane-Air Flames in Recessed Ducts," *Jet Propulsion*, Jan. 1957, pp. 31–43.

[5] Katta, V. R., and Roquemore, W. M., "Study on Trapped-Vortex Combustor—Effect of Injection on Flow Dynamics," *Journal of Propulsion and Power*, Vol. 14, No. 3, 1998, pp. 273–281.

[6] Hsu, K. Y., Goss, L. P., and Roquemore, W. M., "Characteristics of a Trapped-Vortex Combustor," *Journal of Propulsion and Power*, Vol. 14, No. 1, 1998, pp. 57–65.

[7] Tishkoff, J. M., Drummond, J. P., Edwards, T., and Nejad, A. S., "Future Direction of Supersonic Combustion Research: Air Force/NASA Workshop on Supersonic Combustion," AIAA Paper 97-1017, Jan. 1997.

[8]Ben-Yakar, A., and Hanson, R. K., "Supersonic Combustion of Cross-Flow Jets and the Influence of Cavity Flame-Holders," AIAA Paper 99-0484, Jan. 1999.

[9]Yu, K., Wilson, K. J., Smith, R. A., and Schadow, K. C., "Experimental Investigation on Dual-Purpose Cavity in Supersonic Reacting Flows," AIAA Paper 98-0723, Jan. 1998.

[10]Baurle, R. A., and Gruber, M. R., "A Study of Recessed Cavity Flowfields for Supersonic Combustion Applications," AIAA Paper 98-0938, Jan. 1998.

[11]Segal, C., Owens, M. G., Tehranian, S., and Vinogradov, V., "Flameholding Configurations for Kerosene Combustion in a Mach 1.8 Airflow," AIAA Paper 97-2888, July 1997.

[12]Rossiter, J. E., "Wind-Tunnel Experiments on the Flow over Rectangular Cavities at Subsonic and Transonic Speeds," *Aeronautical Research Council Reports and Memo*, No. 3438, London, Oct. 1964.

[13]Yu, K. H., Schadow, K. C., and Smith, R. A., "Enhancement of Flow Mixing by a Frequency Tunable Cavity," U.S. Patent 5520459, May 1996.

[14]Yu, K. H., and Schadow, K. C., "Cavity-Actuated Supersonic Mixing and Combustion Control," *Combustion and Flame*, Vol. 99, 1994, pp. 295–301.

[15]Yu, K. H., Smith, R. A., Wilson, K. J., and Schadow, K. C., "Effect of Excitation on Supersonic Jet Afterburning," *Combustion Science and Technology*, Vols. 113–114, 1996, pp. 597–612.

[16]Zhang, X., and Edwards, J. A., "An Experimental Investigation of Supersonic Flow over Two Cavities in Tandem," *AIAA Journal*, Vol. 30, No. 5, 1992, pp. 1182–1190.

[17]Yu, K. H., and Schadow, K. C., "Role of Large Coherent Structures in Turbulent Compressible Mixing," *Experimental Thermal and Fluid Science*, Vol. 14, 1997, pp. 75–84.

[18]Chinzei, N., Masuya, G., Komuro, T., Murakami, A., and Kudou, K., "Spreading of Two-Stream Supersonic Turbulent Mixing Layers," *Physics of Fluids*, Vol. 29, No. 5, 1986, pp. 1345–1347.

[19]Goebel, S. G., and Dutton, J. C., "Velocity Measurements of Compressible, Turbulent Mixing Layers," AIAA Paper 90-0709, Jan. 1990.

[20]Clemens, N. T., and Mungal, M. G., "Two- and Three-Dimensional Effects in the Supersonic Mixing Layer," *AIAA Journal*, Vol. 30, No. 4, 1992, pp. 973–981.

[21]Hall, J. L., Dimotakis, P. E., and Rosemann, H., "Experiments in Nonreacting Compressible Shear Layers," *AIAA Journal*, Vol. 31, No. 12, 1993, pp. 2247–2254

[22]Powell, A., "On the Mechanism of Choked Jet Noise," *Proceedings of the Physical Society*, London, Vol. 66, 1953, pp. 1039–1056.

[23]Tam, C. K. W., "The Acoustic Modes of a Two-Dimensional Rectangular Cavity," *Journal of Sound and Vibration*, Vol. 49, No. 3, 1976, pp. 353–364.

[24]Tam, C. K. W., and Block, P. J. W., "On the Tones and Pressure Oscillations Induced by Flow over Rectangular Cavities," *Journal of Fluid Mechanics*, Vol. 89, 1978, pp. 373–399.

[25]Raman, G., Envia, E., and Bencic, T. J., "Tone Noise and Nearfield Pressure Produced by Jet-Cavity Interaction," AIAA Paper 99-0604, Jan. 1999.

[26]Heiser, W. H., and Pratt, D. T., *Hypersonic Airbreathing Propulsion*, AIAA, Washington, DC, 1994, pp. 334–339.